Signal Enhancement of Lead and Thallium in Inductively Coupled Plasma Atomic Emission Spectrometry Using On-line Anodic Stripping Voltammetry

Jack R. Pretty* and Joseph A. Caruso†
Department of Chemistry, University of Cincinnati, Cincinnati, OH 45221-0172, USA

An on-line anodic stripping voltammetric (ASV) flow cell was employed for the preconcentration and signal enhancement of transition metals, which exhibit relatively high detection limits in inductively coupled plasma atomic emission spectrometry but which are also responsive in ASV. Signal enhancements of over 60-fold for 20 ml samples of thallium(I) and lead(II) were obtained in much less time than enhancements previously reported for cadmium using this method. The precision was acceptable and plots of peak heights and areas *versus* mass of analyte were linear for thallium and lead. Plots of enhancement factor *versus* sample volume were also linear for both metals.

Keywords: *Inductively coupled plasma atomic emission spectrometry; anodic stripping voltammetry; signal enhancement; preconcentration; lead and thallium determination*

Since its introduction for analytical purposes, inductively coupled plasma atomic emission spectrometry (ICP-AES) has proved to be an excellent method for the identification and determination of the majority of elements.[1-3] This is partly due to the relative ease with which simultaneous multiple element analyses can be performed.[1] The ICP-AES detection limits are suitable for a wide variety of applications. However, for several elements of considerable analytical interest, the detection limits are still relatively poor,[4] owing to the lower emission intensities that they exhibit in the plasma. Among the most important of these elements are lead, thallium, bismuth, tin and mercury. The detection limits for such analytes are often too poor to permit accurate determination of the levels present in biological and environmental systems.[5] Superior detection limits can generally be achieved with techniques such as inductively coupled plasma mass spectrometry, but the instrumental cost is considerably higher, greater expertise is required on the part of operators and sample matrices can exert complex influences on the analyte signal.[3,6-9]

Various techniques have been used to enhance the analyte signals in ICP-AES, including ultrasonic nebulization,[2] hydride generation,[10] preconcentration on resin columns with elution,[5,11] precipitation with collection and redissolution,[12] direct sample insertion[11,13] and electrothermal vaporization (ETV).[2,14] The degree of enhancement reported for these approaches ranges from under one to over three orders of magnitude. The greatest enhancements are predictably achieved with systems that circumvent the limitations of solution nebulization, and that deliver analyte essentially quantitatively to the plasma (hydride, ETV, insertion). Additional enhancement is obtained when preliminary analyte preconcentration is combined with quantitative delivery.[11] The degree to which matrices affect analytical results or convenience of operation varies considerably, as does the over-all instrumental complexity and sample throughput of these procedures.

Many of the transition metals that have relatively poor ICP-AES detection limits are responsive in anodic stripping voltammetry (ASV).[4,15,16] Among the advantages of the latter technique is the potential for preconcentration of trace levels of analyte from a substantial sample volume into a much smaller volume (that of the working electrode).[15,16] Previous reports have described the use of ASV flow cells, based on a working electrode of reticulated vitreous carbon (RVC), placed on-line with the ICP for the purpose of preconcentrating electroactive analytes[17] while eliminating undesirable matrix constituents.[18] The ASV cell designed in these laboratories has been successfully interfaced with both ICP-AES and ICP-MS units.[18-20] Accurate determination of several important metals in certified samples has been demonstrated using the ASV flow system with ICP-MS detection, and large amounts of common matrices that are generally detrimental in ICP have been eliminated to allow improved analyte determination (although certain matrices can exert effects on the electrochemical procedure). Early work also demonstrated the high degree of signal enhancement that could be attained using this cell,[18] as analyte from up to 20 ml of sample was deposited at the electrode, then released into about 300 μl of solution for delivery to an ICP. Following improvements to the system manifold[20] and tests with a variety of electrode surfaces and electrolytes, the use of on-line ASV for improved detection of transition metals, which have relatively poor sensitivity in ICP-AES, was explored. Thallium and lead, both of continuing interest owing to their toxicity and widespread occurrence in biological and environmental systems, were chosen as the test analytes because of their well characterized behaviour in ASV.[15,16,21]

Experimental

Instrumentation

The ICP-AES instrument and microcomputer control system have been described previously.[18] The operating conditions for the ICP-AES instrument are listed in Table 1. Details of the construction and operation of the ASV flow cell have been reported, along with the method for plating of the RVC working electrode with mercury.[18] The flow system manifold incorporated design modifications which are detailed in a separate report.[20] A PAR 174 potentiostat (Princeton Applied Research, Princeton, NJ, USA) was used to control the working electrode potential.

Sample injection was performed using a PTFE valve (No. 5041, Rheodyne). Sample loop volumes were 1.00 ml (Rheodyne) and 2.04 and 4.95 ml (made in our laboratory from the same PTFE tubing as used in the ASV system manifold). The larger sizes were used to minimize the number of loop re-loadings necessary to deliver larger sample volumes. Short lengths of poly(tetrafluoroethylene) (PTFE) tubing built into the injection valve connected it to each end of the sample loop. The volume of liquid contained in this connecting tubing was found to be 100 μl,

*Present address: National Institute of Occupational Safety and Health, 4676 Columbia Parkway, Cincinnati, OH 45226, USA.
†To whom correspondence should be addressed.

Table 1 Operating conditions for ICP-AES instrument

Radiofrequency power	
Forward	1.0 kW
Reflected	<5 W
Gas flow rates	
Coolant	14.4 l min^{-1}
Auxiliary	0.7 l min^{-1}
Nebulizer	1.05 l min^{-1}
Observed wavelengths	
Thallium	276.787 nm
Lead	220.353 nm
Observation height	15 mm above load coil
Monochromator slits	50 μm (entrance and exit)

and this extra volume was included with each sample injection (*e.g.*, four loadings of the 4.95 ml loop also introduced an additional 400 μl of sample into the ASV cell, for a total of 20.2 ml). These extra volumes are reflected in the values quoted in the tables for volumes and mass of analyte. Exact volumes of loops and tubing were determined by filling them with water and draining the contents into a vessel on a balance.

Data Processing

The software which provided monochromator control also allowed the calculation of peak area and height values. The integration time for each ICP-AES data point was 1 s. To assign a baseline intensity value for use in peak integration and further calculations, 20 points on each side of a peak were averaged and the two means were averaged. Integration limits were set by placing cursors on either side of the peak at points on the baseline which most nearly matched the average baseline value, and which were as close as possible to the sides of the peak as observed on the system CRT display. The software then integrated the peak area and displayed the result. The highest peak data point can be found using another software command while the peak is still within the cursors. The mean baseline value is subtracted from the reported maximum to yield peak height. No units are provided with the displayed signal values. The software also includes a Savitsky–Golay smoothing program which was utilized in the present work. Values of 3σ of the baseline (for use in determining analyte detection limits) were determined from 20 or more successive baseline data points as mentioned above.

Reagents

Distilled, de-ionized water, supplied by a purification system (Barnstead, Boston, MA, USA), was used for all solutions. Doubly distilled nitric acid (No. 621, GFS Chemicals, Columbus, OH, USA) was used for the sample electrolyte and the supply electrolyte delivered to the ASV cell (both 0.1 mol l^{-1}) and for the bypass solution which was supplied to the ICP whenever the cell output was diverted (1% v/v). The mercury plating solution was 1 mmol l^{-1} in mercury(II) nitrate (99.999%, Alfa Products, Morton Thiokol, Danvers, MA, USA), prepared in 0.1 mol l^{-1} ammonium nitrate of 99.999% purity (No. 25,606-4, Aldrich, Milwaukee, WI, USA). Stock solutions (10 μg ml^{-1}) of thallium and lead were prepared from standard solutions of each element (Fisher Scientific, Cincinnati, OH, USA) and diluted as needed to prepare samples. All samples of less than 100 ng ml^{-1} analyte concentration were prepared fresh daily.

Results and Discussion

Optimization of Flow Rate and Timing

Previous experiments involving signal enhancement (of cadmium in 0.1 mol l^{-1} NH_4NO_3) had used relatively low rates of sample delivery to the ASV cell in order to ensure high deposition efficiency. This resulted in considerable enhancement of the ICP-AES signal (up to a factor of 50 for 20 ml samples), but inordinately long times were required for larger samples.[18] This was clearly unacceptable for routine application, and one goal of the present work was to improve throughput for large sample volumes. Several experiments with analytes such as copper and arsenic in dilute nitric acid electrolyte[19] have indicated that substantial enhancement could be achieved at higher flow rates than those used previously. Hence, the reduction in analyte deposition efficiency at faster flow rates could be more than offset by the larger sample volume that could be run per unit time. It was presumed that the high conductivity of nitric acid solutions promoted efficient deposition at faster flow rates, so 0.1 mol l^{-1} HNO_3 was used as the sample and cell supply electrolytes in experiments with lead and thallium. Although both analytes may be deposited on the surface of a bare carbon working electrode, a mercury-coated electrode was used, as results for earlier experiments had indicated that this electrode often gave superior precision.[19,20] In all optimization and enhancement studies, the ASV cell was flushed with clean electrolyte for 2 min after passage of the sample before the deposited analytes were stripped.

Using 4 ml volumes of 1 μg ml^{-1} thallium as test samples, preliminary experiments were carried out to determine how rapid a sample delivery flow rate could be used without an inordinate decrease in the analyte deposition efficiency, as demonstrated by the size of the ICP-AES signal peak. At each flow rate, the effect of allowing different lengths of time for complete passage of the 4 ml sample volume through the ASV cell was examined. It was found that a sample delivery rate of 1.58 ml min^{-1} gave peak heights equal to those achieved at slower flow rates, and better than those achieved at faster flow rates. At this deposition flow rate, allowing 4 min per sample (equivalent to 1 min ml^{-1}) gave the best response per unit time; allowing less time per volume reduced the peak heights substantially, whereas allowing more time produced very minor peak height gains which were offset by the lower sample throughput. The need to allow more time for sample passage than might seem apparent from the flow rate is due to broadening of the sample plug as it moves through the ASV flow system manifold. The flow and time parameters listed above were used for the remaining signal enhancement studies. Counting the time for reloading the 5 ml sample loop, a 20 ml sample required 22 min to be run through the ASV cell. In the previously reported work with cadmium, more than 1 h had been required for the same volume.[18]

Thallium

Thallium was deposited at the electrode at −1.0 V, and a final potential of −0.2 V was used for stripping. Analyte levels ranging from 1 μg ml^{-1} to 50 ng ml^{-1} were run using various total volumes. Because of this, a total sample mass of 1010 ng of Tl was delivered to the ASV cell in two ways: as 10.1 ml of 100 ng ml^{-1} Tl and as 20.2 ml of 50 ng ml^{-1} Tl. Therefore, two data points were obtained for this mass of analyte. This provided a greater number of points for the generation of plots and allowed a comparison of the values obtained for the same mass of thallium using different sample volumes and total deposition times. For the pair of 1010 ng values, the peak heights matched very well, whereas the peak areas differed slightly (Table 2). An

Table 2 Signal enhancement of thallium in ICP-AES. Peak heights (arbitrary units) and areas (s), RSD values (%) in parentheses. Three replicate runs made for all samples; sample concentrations in ng ml^{-1} with volumes (ml) given in parentheses

Sample	Mass of Tl/ ng	Mean peak height	Mean peak area/s
1* (4.28)	4280	1.67 (1.2)	1.16 (2.2)
500 (4.28)	2140	0.84 (6.3)	0.550 (1.7)
100 (5.05)	505	0.20 (10)	0.146 (4.1)
500 (10.10)	5050	2.05 (1.4)	1.5 (1.5)
100 (10.10)	1010	0.44 (4.9)	0.316 (1.7)
100 (20.20)	2020	0.83 (4.5)	0.615 (1.2)
50 (20.20)	1010	0.44†	0.336 (4.9)

*Value given in μg ml^{-1}.
†All replicate runs were calculated to have the same value.

unexpected result was obtained for 2020 and 2140 ng; the peak height values are approximately in the expected proportions (within the level of precision), but the peak area found for the lower mass of analyte is significantly greater than that found for the higher mass.

The parameters for plots of peak height and area *versus* mass of thallium were as follows (units for height are arbitrary and area is given in seconds): peak height *versus* mass of analyte, correlation coefficient=0.99913, slope=0.3955 s μg^{-1} Tl, intercept=0.0208; peak area *versus* mass of analyte, correlation coefficient=0.99614, slope=0.276 s μg^{-1} Tl, intercept=0.0235 s. Both plots are essentially linear, the peak-height plot being the better of the two according to the correlation coefficients. The peak area anomaly mentioned above was probably partly responsible for this. The small non-zero intercept values may be the result of the uncertainty in assigning an exact baseline value owing to the presence of baseline noise (see under Data Processing). This can influence the integration of the smallest peaks (it is also one probable reason for the poorer RSD values associated with some of the smaller peaks). No RSD value is reported for the peak height of 20 ml of 50 ng ml^{-1} Tl because the data processing software gave the same value for all three replicate runs, an artifact of the digitization process.

For the ICP-AES system used in this work, the continuous nebulization detection limit of thallium (comparing 3σ of the baseline to the height of the signal for 1 μg ml^{-1} Tl) was 6.4×10^2 ng ml^{-1} at the emission wavelength of 276.79 nm. Running various volumes of supporting electrolyte blank through the ASV cell gave no thallium peak signals in ICP, so the ASV–ICP detection limit could not be calculated as three times the standard deviation of electrolyte blank peak area. Based on the height of the ASV–ICP peaks obtained by preconcentrating 20 ml of 50 ng ml^{-1} Tl, the detection limit calculated using 3σ of the baseline was 11 ng ml^{-1} for a 20 ml sample volume. After application of a nine-point smoothing program, the 3σ detection limit was 233 ng ml^{-1} by continuous nebulization and 4.5 ng ml^{-1} for 20 ml samples using the ASV cell. The use of larger sample volumes would further lower the ASV–ICP detection limits.

Lead

Lead was also deposited at −1.0 V with a final stripping potential of −0.2 V. As with thallium, running different volumes of supporting electrolyte blank through the ASV cell gave no visible analyte peak signals above the baseline in ICP-AES. Various volumes of lead sample, at levels ranging from 1 μg ml^{-1} to 50 ng ml^{-1} of lead, were delivered to the cell, so that pairs of data points resulted for two masses of analyte (1010 and 5050 ng). For both of these pairs, the peak heights and areas matched very well (Table 3). Only one 20.2 ml volume of 100 ng ml^{-1} of lead (2020 ng) was made owing to time constraints, and the height and area values for this single run were omitted when the plots for peak height and area *versus* analyte mass were generated. The RSD values for peak heights and areas ranged from low to moderately large, with values for area often much lower than the corresponding values for height, and lower analyte masses generally exhibiting larger RSD values (Table 3).

As observed for thallium, the plot of mass analyte *versus* peak area is less linear than that for mass *versus* peak height. The parameters for the plots were as follows (units for height are arbitrary and area is give in seconds): peak height *versus* mass of analyte (omitted 2.15 for 2020 ng Pb), correlation coefficient=0.99979, slope=0.962 s μg^{-1} Pb, intercept=0.139; peak area *versus* mass of analyte (omitted 1.99 for 2020 ng Pb), correlation coefficient=0.99689, slope=0.701 s μg^{-1} Pb, intercept=0.286 s.

Table 3 illustrates several peak area discrepancies. Whereas the peak heights for 2020 and 2525 ng of lead were in proportion, the peak area of the lower mass was slightly higher than that of the other. The area value for 1100 ng lead was also unexpectedly high, although the peak height was proportional (within the level of precision) to that of other analyte masses. This was the only example in which a sample volume of about 1 ml was used, and the high value could indicate that the brief deposition time required for this small volume allowed a slightly greater proportion of lead to be retained at the electrode prior to stripping (less chance for the analyte to redissolve back into the dilute nitric acid supply electrolyte flowing through the cell), relative to that retained using larger samples and longer deposition times. However, if this were so, the mean value of peak height should also have been affected.

Both peak height and peak area plots exhibited fairly high positive intercept values. The reasons for this are unknown, as runs of the electrolyte blank produced no significant peak signals. One possibility is that the ASV cell was not functioning at maximum efficiency for the higher masses of analyte, yielding disproportionately small peaks for larger masses of analyte and causing the slopes of the plots to be artificially lowered. This could occur if the amount of lead introduced into the cell exceeded the amount of lead that could dissolve in the mercury film, although the large surface area available with the mercury-coated RVC working electrode makes this appear unlikely. Thallium is more soluble in mercury than lead, so exceeding the solubility limit would be less likely for the former.[15] However, the good linearity of the peak height curve for lead does not indicate a disproportionate deposition efficiency for higher masses of analyte.

For the ICP-AES system used in this work, the detection limit of lead with continuous nebulization (determined as above for thallium using 3σ of the baseline) was 4.9×10^2 ng ml^{-1} without smoothing. The 3σ detection limit based on the height of ASV–ICP peaks produced from 20 ml of 50 ng ml^{-1} Pb was 7.9 ng ml^{-1}. After nine-point data smoothing, the respective values were 221 and 3.5 ng ml^{-1}.

Signal Enhancement Capability

The performance of the ASV–ICP system in signal enhancement is summarized in Table 4, by comparing the continuous nebulization signal heights for the indicated analyte levels with peak heights obtained with various volumes of the same analyte levels using the ASV flow system. The enhancement factor is defined as the ratio of the height of the ASV–ICP peak signal for a given volume of analyte to the height of the ICP-AES continuous nebulization signal produced by the same analyte level. For analyte levels that

Table 3 Signal enhancement of lead in ICP-AES. Peak heights (arbitrary units) and areas (s), RSD values (%) in parentheses. Three replicate runs made for all samples except as indicated; sample concentrations in ng ml^{-1} with volumes (ml) given in parentheses

Sample	Mass of Pb/ng	Mean peak height	Mean peak area/s
1* (1.10)	1100	1.15 (7.1)	1.26 (0.75)
1* (5.05)	5050	5.01 (2.0)	3.84 (0.96)
500 (5.05)	2525	2.55 (1.6)	1.93 (0.88)
500 (10.10)	5050	4.99 (2.7)	3.84 (0.64)
100 (10.10)	1010	1.16 (4.6)	0.977 (0.55)
50 (10.10)	505	0.59 (5.6)	0.527 (3.80)
50 (20.20) (2 runs)	1010	1.14, 1.17	0.967, 1.07
100 (20.20) (1 run)	2020	2.15	1.99

*Values given in μg ml^{-1}.

were above the continuous nebulization detection limits, direct calculation of enhancement factors was possible. For levels that were below the detection limit, the values listed in Table 4 for continuous nebulization signal height were calculated based on the heights of signals observed for detectable levels, and these calculated height values were used in determining the enhancement factors.

If the enhancement factor is plotted against sample volume, the slope of the plot can be taken as the signal enhancement capability of the ASV flow system, defined as enhancement factor per millilitre of sample. For both thallium and lead, the resulting plots were reasonably linear, although both also exhibit small negative intercepts for unknown reasons (Table 4). The slopes of the plots were 3.31 for both analytes while the average enhancement factor was 65.6 for samples of just over 20 ml volume, attesting to the efficiency of the ASV flow cell in the signal enhancement of these metals.

The performance of the systems is illustrated by Figs. 1 and 2. Both figures present continuous nebulization signals for levels of analyte that could be observed without the ASV cell alongside ASV–ICP peaks resulting from 20 ml volumes of analytes at levels that were well below the continuous nebulization detection limits of the available ICP-AES unit. Fig. 1 shows two replicate peaks for 20 ml of 50 ng ml^{-1} of thallium and Fig. 2 shows a single run for 20 ml of 100 ng ml^{-1} of lead. Although no data smoothing was used on these displays, the ASV–ICP peaks are visible well above the baseline noise. As indicated numerically in Table 4, the peak heights are well above the continuous nebulization signals for 1 μg ml^{-1} of the respective analytes.

Conclusions

The ICP-AES unit used in this work could not provide fully optimized analyte signals. Further, the available photomultiplier tube was unresponsive at the most sensitive thallium emission wavelength (190.864 nm) (ref. 4) and a less intense line was monitored instead. For these reasons, the detection limits quoted for the analyte metals with continuous nebulization do not match those which can be obtained under more carefully controlled conditions. However, the degree of signal enhancement obtained for a given sample volume with the on-line ASV cell is not affected by these factors, and interfacing the system with a more sensitive ICP unit would result in proportionally better ASV–ICP

Table 4 Signal enhancement capability of ASV flow system: ICP-AES signal heights obtained by continuous nebulization compared with heights of peaks obtained by preconcentration of indicated sample volumes. Continuous nebulization values for analyte levels below detection limits are calculated as described in the text. Signal heights in arbitrary units

Analyte Concentration	Continuous nebulization signal height	Sample volume in ASV–ICP/ml	ASV–ICP Peak height	Enhancement factor
Thallium				
10 μg ml^{-1}	1.32			
1 μg ml^{-1}	0.131	4.28	1.67	12.7
500 ng ml^{-1}	0.066	4.28	0.84	13
	(calc.)	10.10	2.05	31
100 ng ml^{-1}	0.013	5.05	0.20	15
	(calc.)	10.10	0.44	34
		20.20	0.83	64
50 ng ml^{-1}	0.0066	20.20	0.44	67
	(calc.)			
Lead				
10 μg ml^{-1}	3.43			
1 μg ml^{-1}	0.342	1.10	1.15	3.37
		5.05	5.01	14.6
500 ng ml^{-1}	0.17	5.05	2.55	15.0
		10.10	4.99	29.4
100 ng ml^{-1}	0.034	10.10	1.16	34.1
	(calc.)	20.20	2.15	63.2
50 ng ml^{-1}	0.017	10.10	0.59	35
	(calc.)	20.20	1.16	68.2

Enhancement factor *versus* sample volume

Thallium: correlation coefficient = 0.99854, slope = 3.31 ml^{-1}, intercept = −1.31
Lead: correlation coefficient = 0.99549, slope = 3.31 ml^{-1}, intercept = −1.01

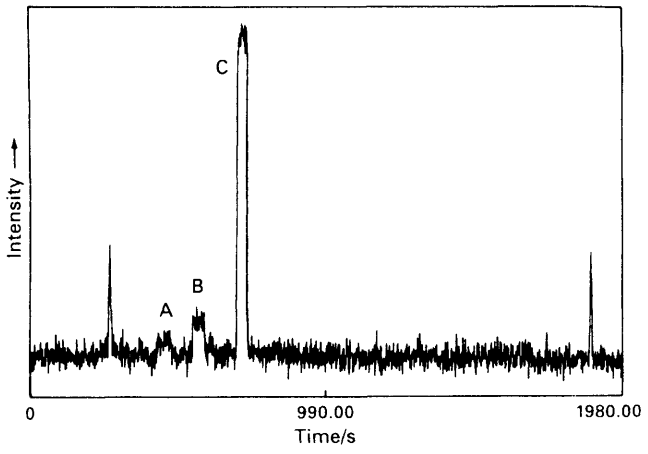

Fig. 1 Peaks resulting from preconcentration of 20 ml of 50 ng ml^{-1} Tl in ASV–ICP-AES. Continuous nebulization signals shown for comparison: A, 500 ng ml^{-1} Tl; B, 1 μg ml^{-1} Tl; and C, 10 μg ml^{-1} Tl. Display has not been smoothed. Further details in text

detection limits than those reported here. The ASV cell itself was not designed specifically for maximum signal enhancement efficiency. Appropriate design modifications or the use of a working electrode with a higher surface area (allowing more efficient analyte deposition at faster flow rates) could further improve the degree of enhancement and sample throughput.

The available ICP-AES detection system allowed only one element at a time to be monitored, and accordingly only single-analyte test solutions were utilized in this work. However, the deposition potential of -1.0 V and final stripping potential of -0.2 V were suitable for both lead and thallium. With a suitable ICP-AES unit as detector, simultaneous element determinations could be performed with the ASV flow system by depositing both elements at once from the sample, then stripping them back into solution together. A similar approach would hold for most of the transition metals that deposit efficiently at a mercury film electrode (zinc, cadmium, copper, indium, *etc.*) so long as suitable deposition and stripping potentials are used.

In determining elements by ASV alone, the simultaneous deposition of metals with similar crystalline structures can lead to the formation of alloy-like intermetallic states within mercury film electrodes.[16] These generally occur

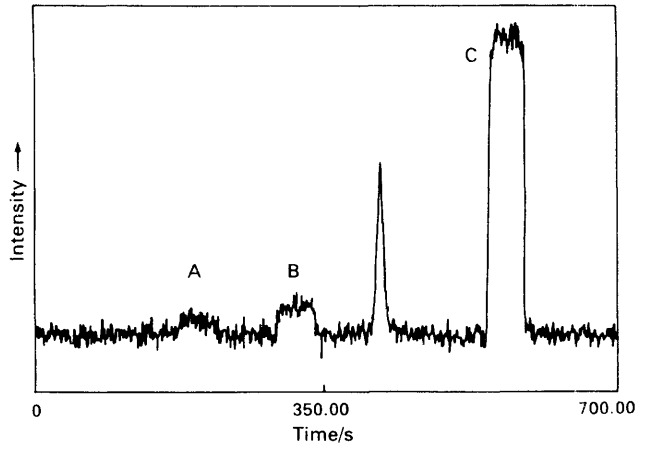

Fig. 2 Peak resulting from preconcentration of 20 ml of 100 ng ml^{-1} Pb in ASV–ICP-AES. Continuous nebulization signals shown for comparison: A, 500 ng ml^{-1} Pb; B, 1 μg ml^{-1} Pb; and C, 10 μg ml^{-1} Pb. Display has not been smoothed. Further details in text

when one of the metals is present at a high concentration within the film and in a much higher proportion than the others. The stripping current peaks of intermetallic states can lie at unexpected potential values and analyte determination by measurement of these peak heights and areas is inaccurate. In the present application, intermetallic formation is theoretically of less importance; as long as all deposited metals are completely stripped from the electrode at the end of the potential scan for delivery to the ICP detector, undistorted, element-specific determinations are possible.

As stated previously, the successful determination of selected analytes in certified samples has been demonstrated.[19,20] Several experimental factors in this work (such as use of a mercury-coated electrode and dilute nitric acid electrolyte) are similar to the conditions successfully employed for the determination of copper in a urine matrix.[20] It is likely that lead and thallium will prove equally amenable to determination by ASV–ICP, although this has not yet been tested with certified samples. When sufficient sample volumes are available, the system can provide a substantial reduction in detection limits while simultaneously eliminating detrimental sample matrix effects.

The efficiency of the on-line ASV–ICP system for signal enhancement of lead and thallium has been demonstrated. The inconsistencies observed for analyte peak area values are of some concern, particularly given the generally superior behaviour of the corresponding peak height data. The reasons for these variations have not yet been elucidated. Possible considerations include the accuracy with which peaks have been integrated, and the question of whether data points were taken often enough to trace adequately the most rapid changes of the ICP-AES peak signal. Alternatively, undetected shifts in various system parameters over the course of extended experimental sessions could affect the final results. The ASV flow system is still a prototype in some respects and imperfect performance is not unexpected.

Experiments similar to those described here have been performed with tin and mercury, but although substantial enhancements were achieved, these analytes require the use of more specialized electrode or electrolyte systems for the best anodic stripping response, and the results to date lie outside the scope of this paper. Although these signal enhancement studies have focused on elements with high ICP-AES detection limits, the approach is equally valid for the signal enhancement of electroactive analytes in ICP-MS, although the magnitude of the blank peak signals produced by trace electrolyte contamination has so far limited exploration of this option.

The potentiostat and *x*–*y* recorder were provided by the National Forensic Center of the Food and Drug Administration, Cincinnati, OH. J.R.P. notes the suggestion of Karen Wolnick of the National Forensic Center that signal enhancement of thallium merited examination. The assistance of Robert Voorheis, Paul MacKensie, William Brauntz, Arthur Case and Douglas Hurd of the electronics and machine shops of the Department of Chemistry, University of Cincinnati, and the advice contributed by Elmo A. Blubaugh are also gratefully acknowledged. Our particular thanks are due to Timothy Davidson, who conceived the project and participated in the planning stages prior to his departure from the laboratory.

References

1 Fassel, V. A., and Kniseley, R. N., *Anal. Chem.*, 1974, **46**, 1110A.
2 Barnes, R. M., *CRC Crit. Rev. Anal. Chem.*, 1978, **7**, 203.
3 Olesik, J. W., *Anal. Chem.*, 1991, **63**, 12A.

4 Winge, R. K., Peterson, V. J., and Fassel, V. A., *Appl. Spectrosc.*, 1979, **33**, 206.
5 Wunsch, G., Knobloch, S., Luck, J., and Blodorn, W., *Spectrochim. Acta, Part B*, 1992, **47**, 199.
6 Hieftje, G. M., and Vickers, G. H., *Anal. Chim. Acta*, 1989, **216**, 1.
7 Tan, S., and Horlick, G., *J. Anal. At. Spectrom.*, 1987, **2**, 745.
8 Tan, S., and Horlick, G., *Appl. Spectrosc.*, 1986, **40**, 445.
9 Vaughan, M. A., and Horlick, G., *Appl. Spectrosc.*, 1986, **40**, 434.
10 Hwang, J. D., Huxley, H. P., Diomiguardi, J. P., and Vaughn, W. J., *Appl. Spectrosc.*, 1990, **44**, 491.
11 Moss, P., and Salin, E. D., *Appl. Spectrosc.*, 1991, **45**, 1581.
12 Akagi, T., and Haraguchi, H., *Anal. Chem.*, 1990, **62**, 81.
13 Abdullah, M., Fuwa, K., and Haraguchi, H., *Appl. Spectrosc.*, 1987, **41**, 715.
14 Nisamaneepong, W., Caruso, J. A., and Ng, K. C., *J. Chromatogr. Sci.*, 1985, **23**, 465.
15 Vydra, F., Stulik, K., and Julakova, E., *Electrochemical Stripping Analysis*, Ellis Horwood, Chichester, 1976.
16 Wang, J., *Stripping Analysis: Principles, Instrumentation and Applications*, VCH, Deerfield Beach, FL, 1984.
17 Ogaram, D. A., and Snook, R. D., *Analyst*, 1984, **109**, 1597.
18 Pretty, J. R., Evans, E. H., Blubaugh, E. A., Shen, W.-l., Caruso, J. A., and Davidson, T. M., *J. Anal. At. Spectrom.*, 1990, **5**, 437.
19 Pretty, J. R., *PhD Dissertation*, University of Cincinnati, 1991.
20 Pretty, J. R., Blubaugh, E. A., Evans, E. H., Caruso, J. A., and Davidson, T. M., unpublished work.
21 Hoeflich, L. K., Gale, R. J., and Good, M. L., *Anal. Chem.*, 1983, **55**, 1591.

Paper 2/00757F
Received February 12, 1992
Accepted January 1, 1993